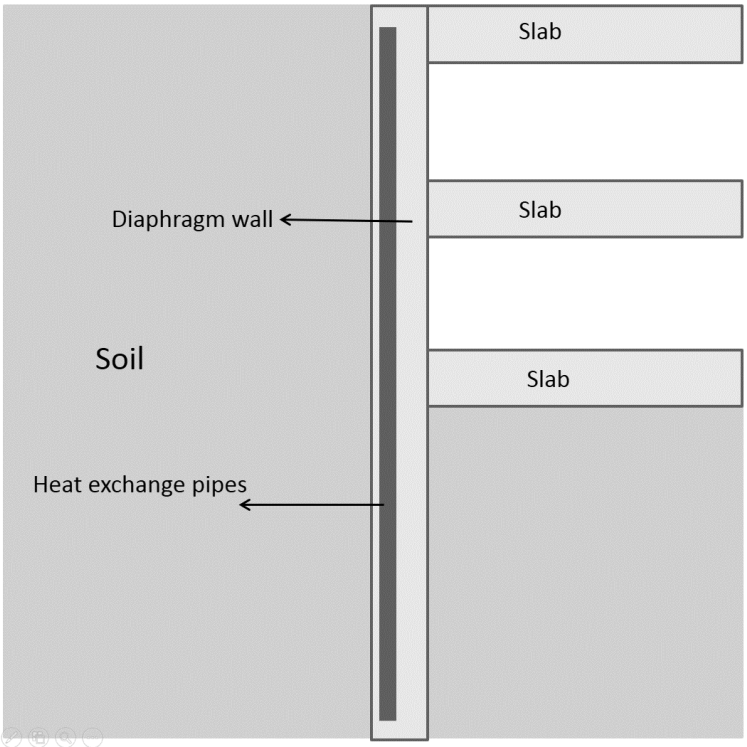

Figure 1. Section plan drawing of geothermal heat exchangers embedded in a diaphragm wall.

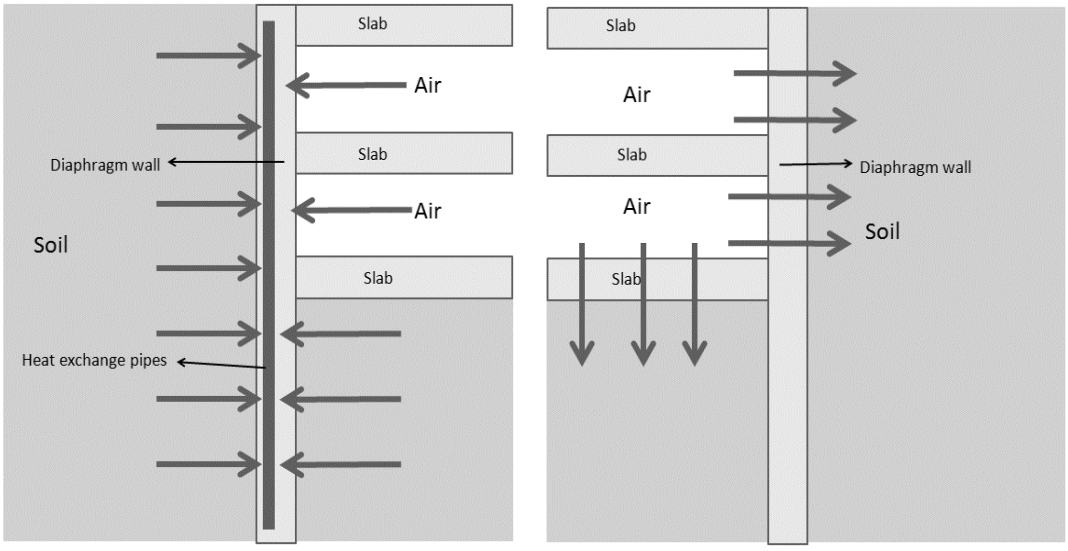

Winter Summer

Figure 2: Heating-only operating mode of thermo-active diaphragm wall

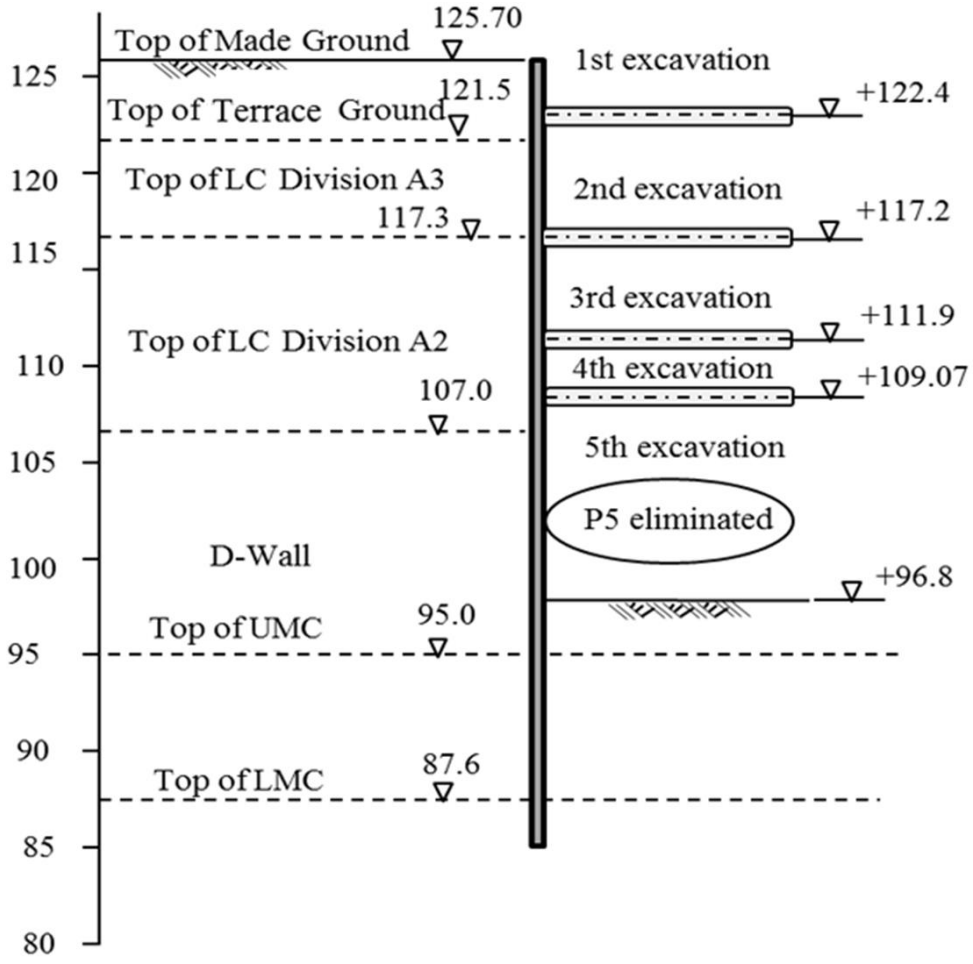

Figure 3. Geometry of Dean Street Station Box

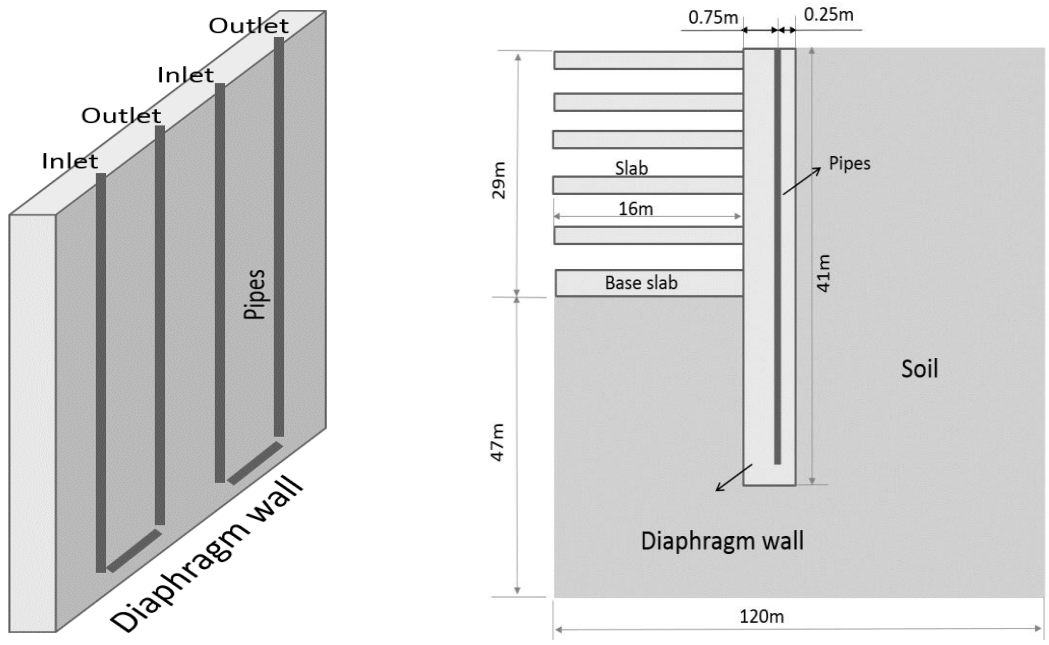

(a)

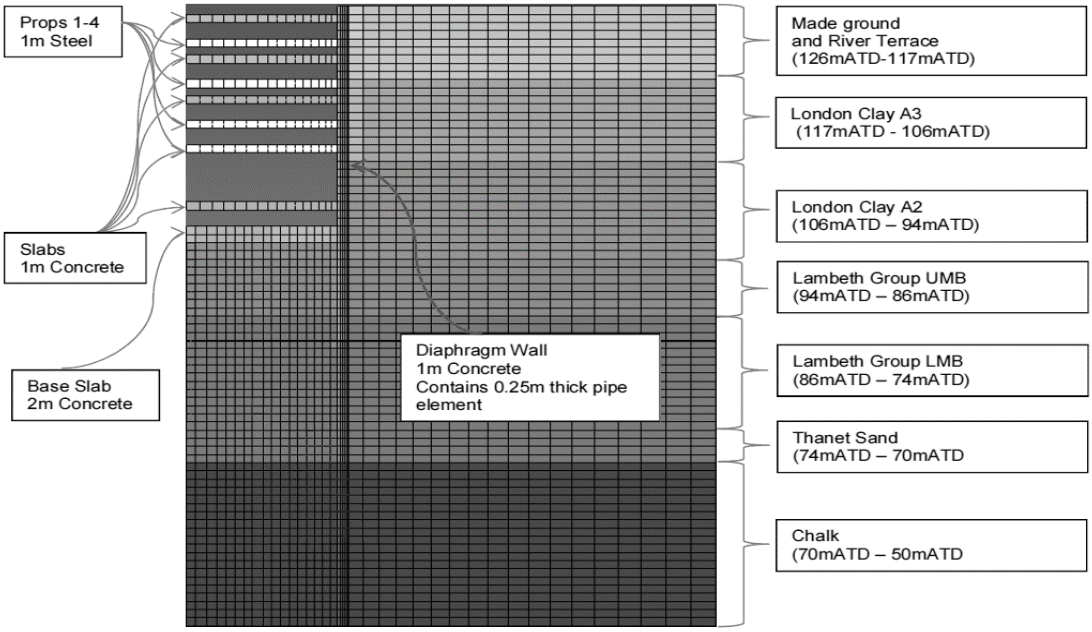

(b)

Figure 4. Finite element model: (a) Geometry; (b) Meshing

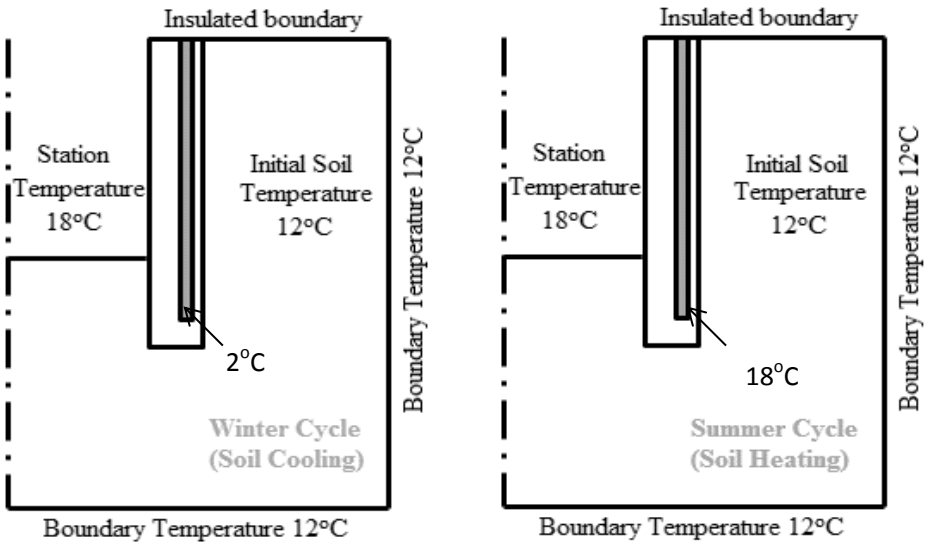

Figure 5. Temperature boundary conditions of the thermo-active diaphragm wall

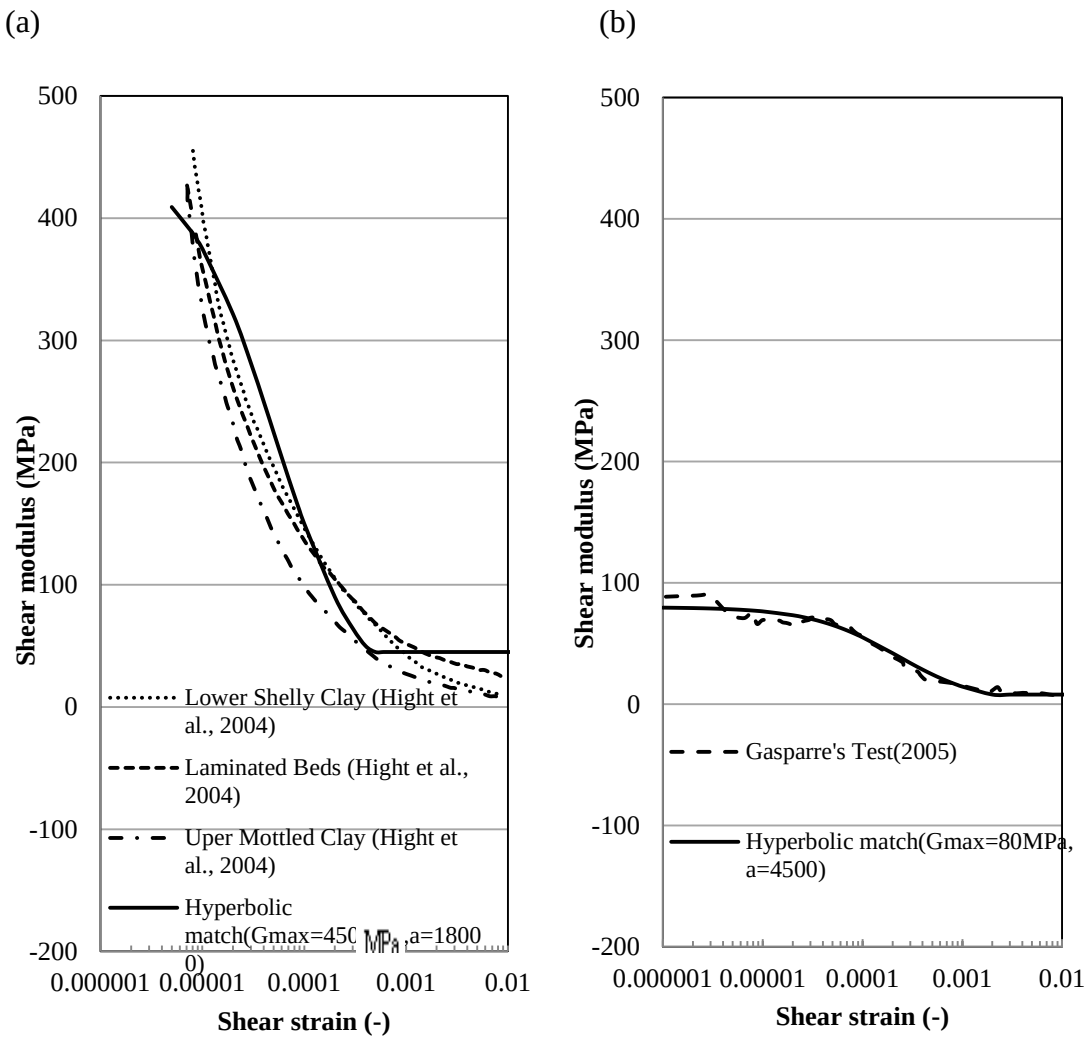

Figure 6. Test data for stiffness degradation and hyperbolic match: (a) London Clay; (b) Lambeth Group（after Schwamb 2014）

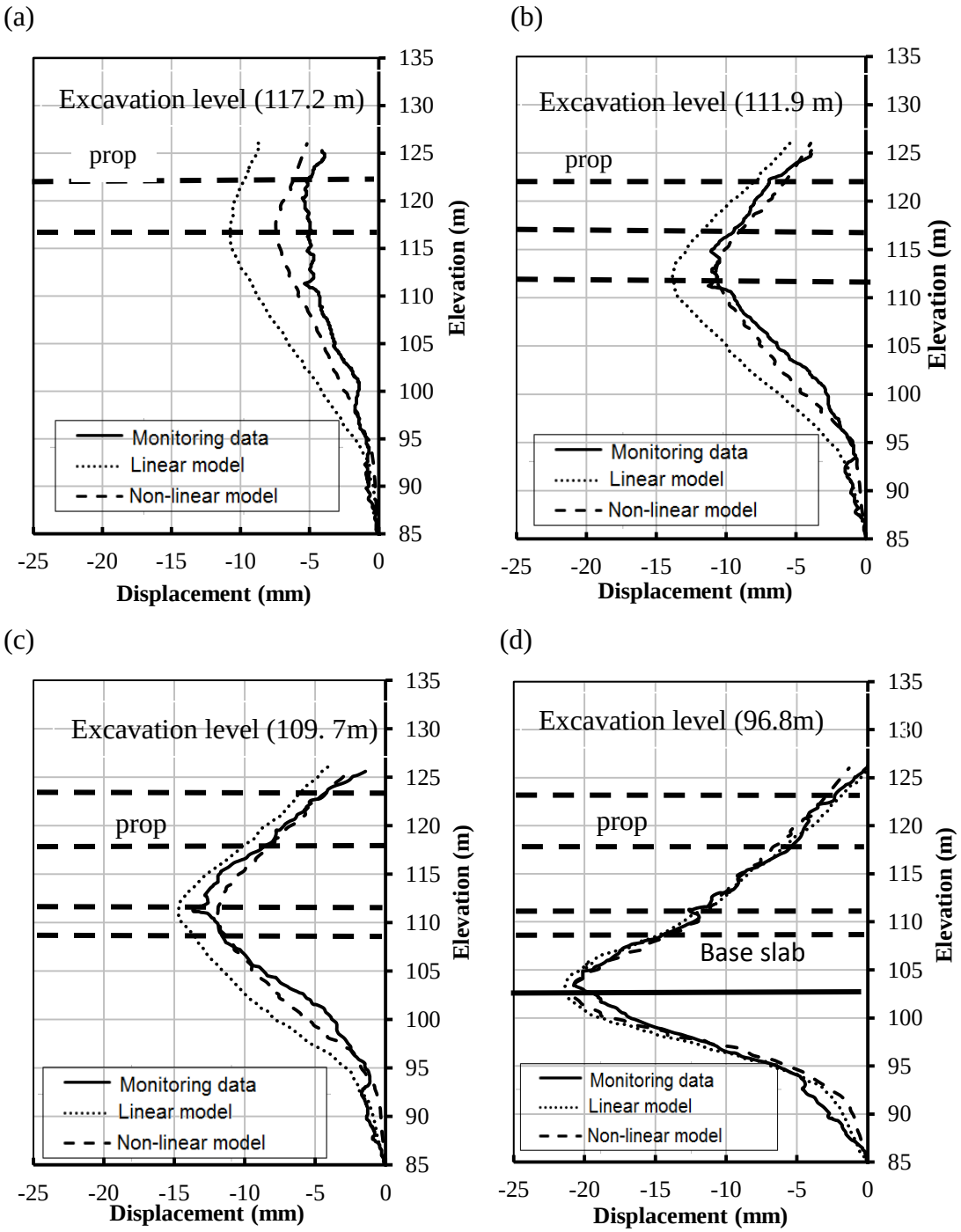

Figure 7. Comparison of the relative horizontal displacements between the linear elastic model and the non-linear elastic model

(a)

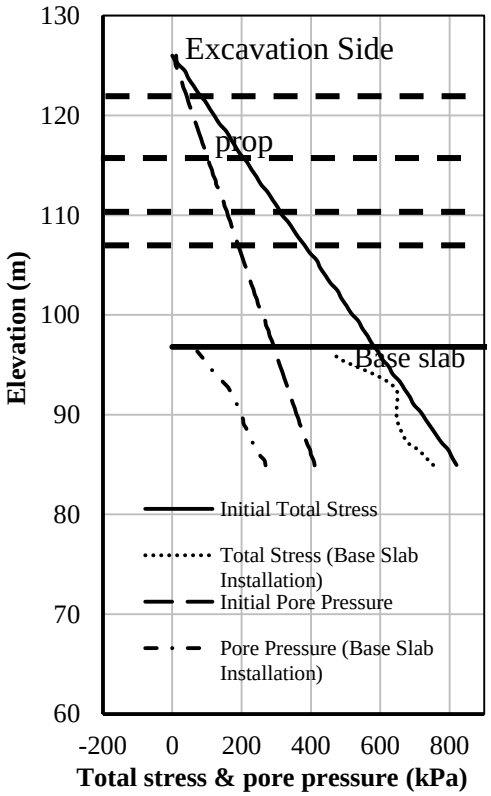
Excavation Side
prop
Base slab
Initial Total Stress
Total Stress (Base Slab Installation)
Initial Pore Pressure
Pore Pressure (Base Slab Installation)
Elevation (m)
Total stress & pore pressure (kPa)

(b)

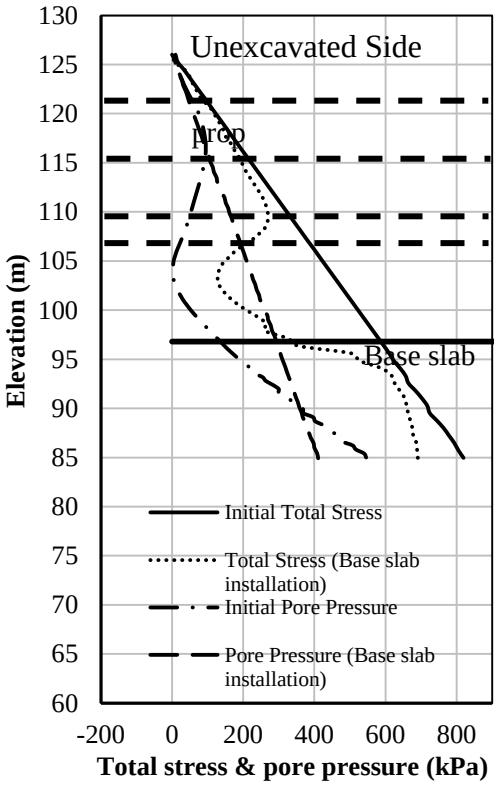
Unexcavated Side
prop
Base slab
Initial Total Stress
Total Stress (Base slab installation)
Initial Pore Pressure
Pore Pressure (Base slab installation)
Elevation (m)
Total stress & pore pressure (kPa)

(c)

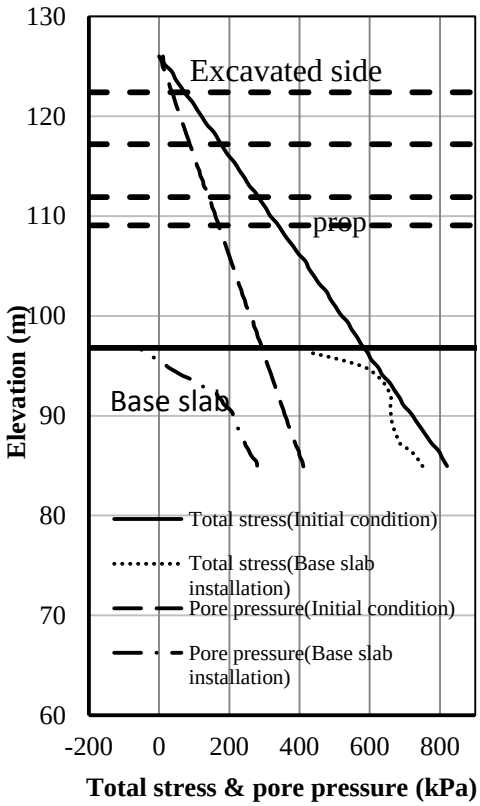
Excavated side
prop
Base slab
Total stress(Initial condition)
Total stress(Base slab installation)
Pore pressure(Initial condition)
Pore pressure(Base slab installation)
Elevation (m)
Total stress & pore pressure (kPa)

(d)

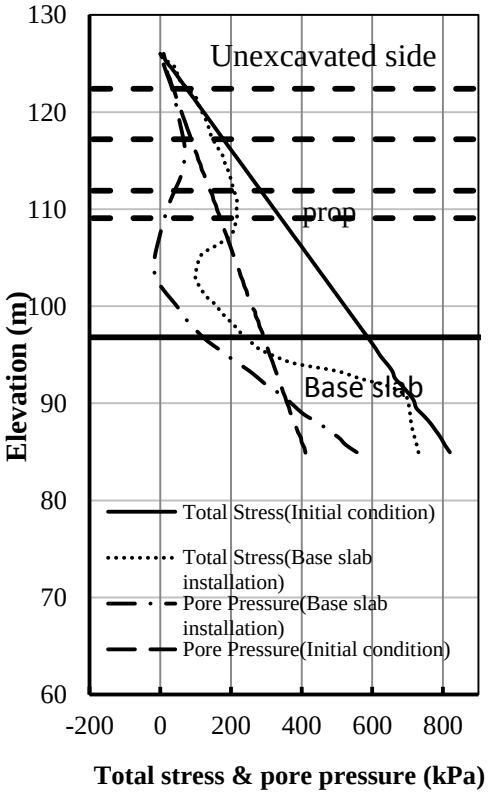
Unexcavated side
prop
Base slab
Total Stress(Initial condition)
Total Stress(Base slab installation)
Pore Pressure(Base slab installation)
Pore Pressure(Initial condition)
Elevation (m)
Total stress & pore pressure (kPa)

Figure 8. Total stress and pore pressure: (a) Excavated side with linear elastic model; (b) Unexcavated side with linear elastic model; (c) Excavated side with non-linear elastic model; (d) Unexcavated side with non-linear elastic model

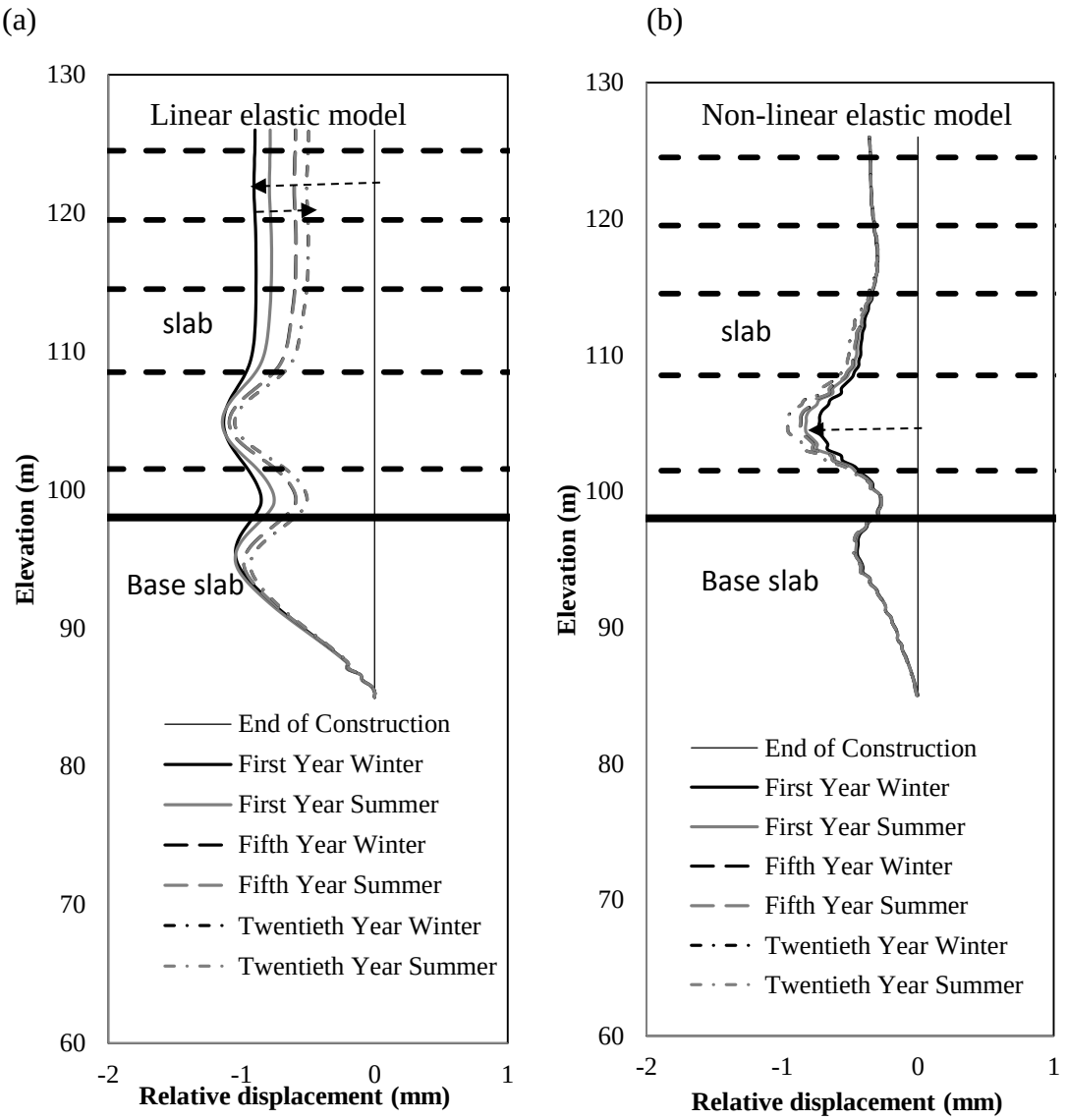

Figure 9. Relative horizontal displacement of the diaphragm wall without operation of the GSHP: (a) Linear elastic model; (b) Non-linear elastic model

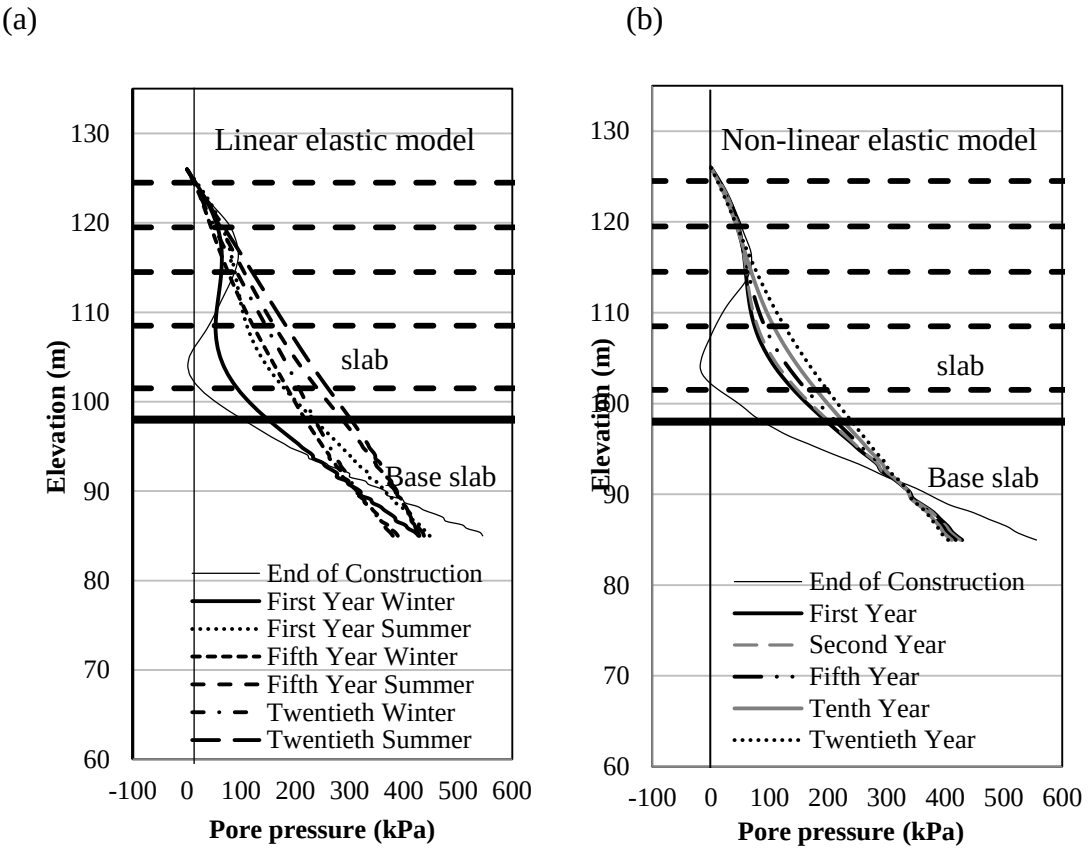

Figure 10. Long-term pore pressure change on the unexcavated side: (a) Linear elastic model; (b) Non-linear elastic model

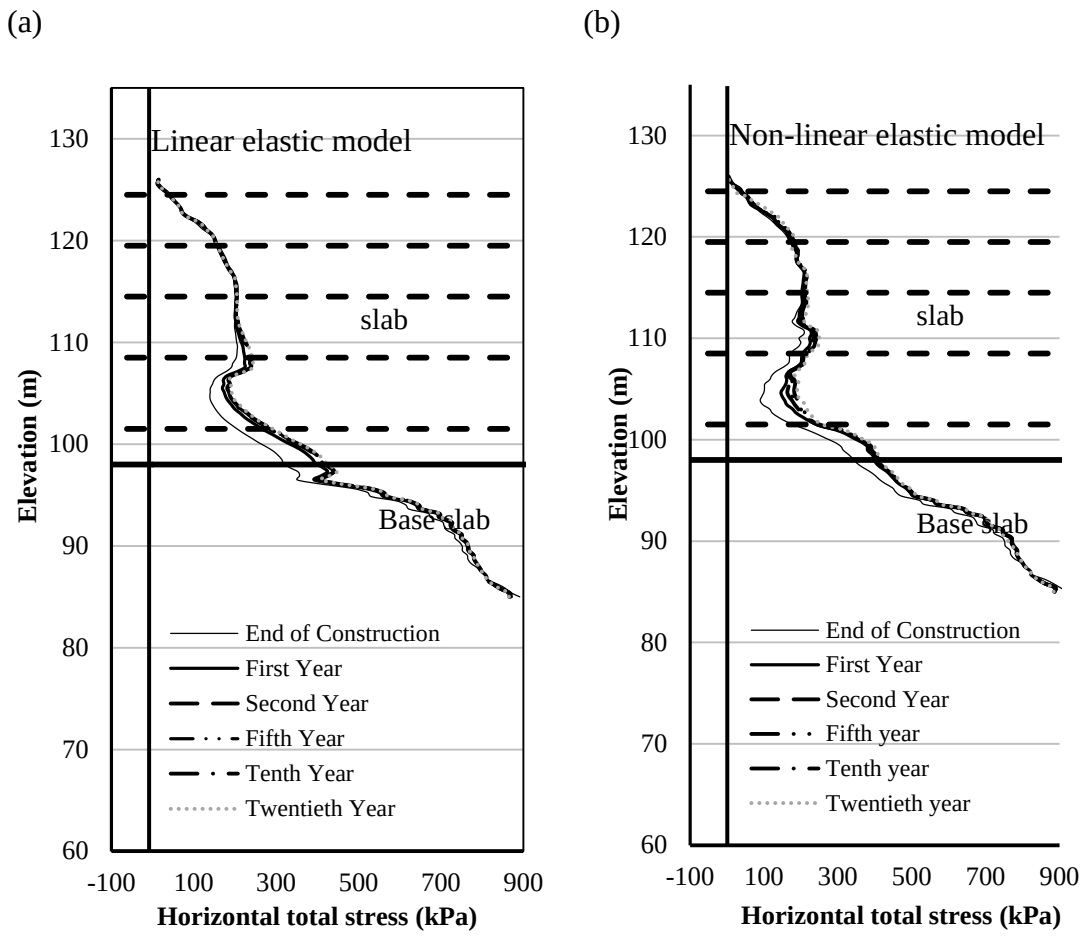

Figure 11. Long-term total stress change on the unexcavated side: (a) Linear elastic model; (b) Non-linear elastic model

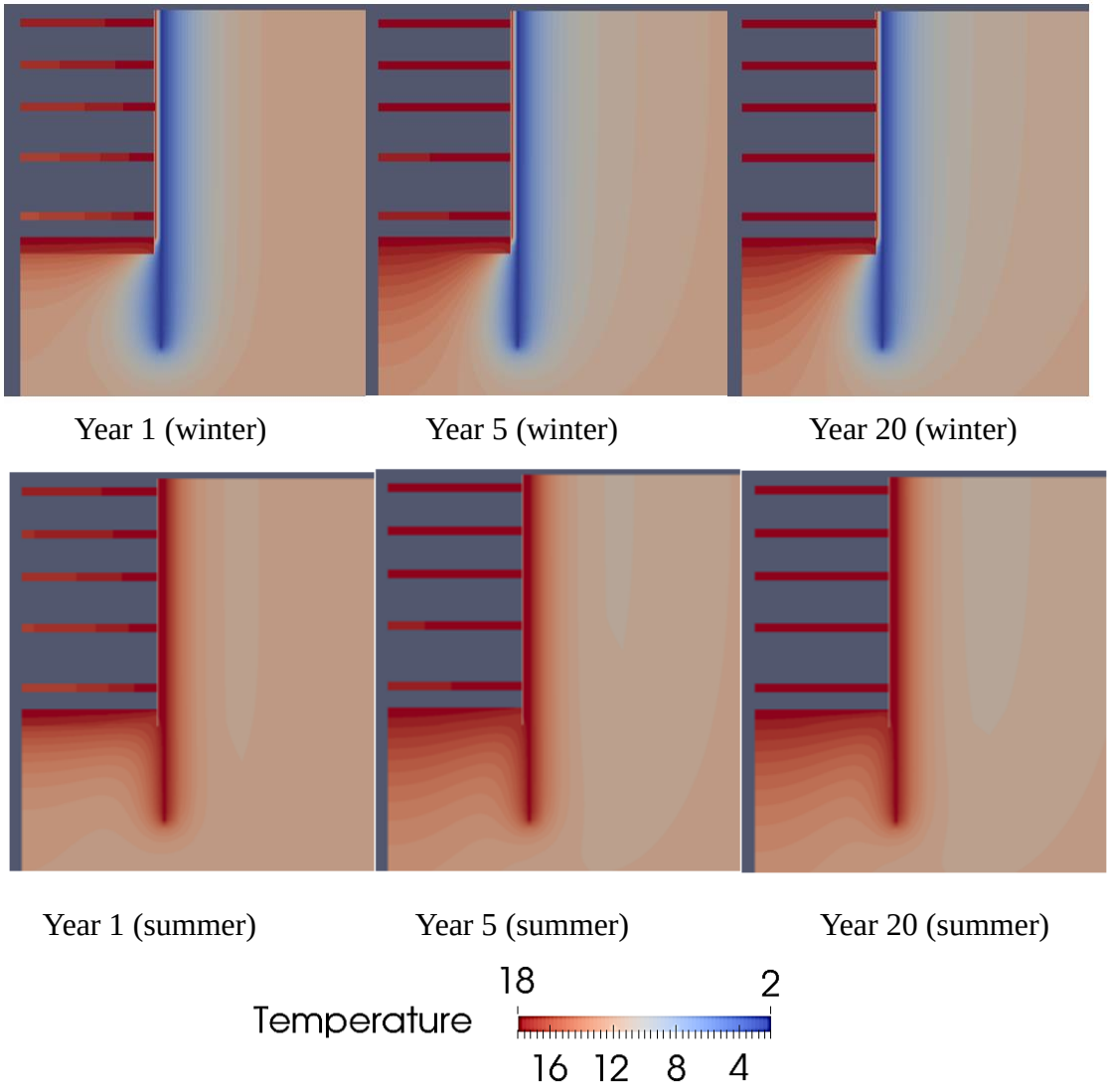

Figure 12. Contours of temperature changes with operation of GSHP

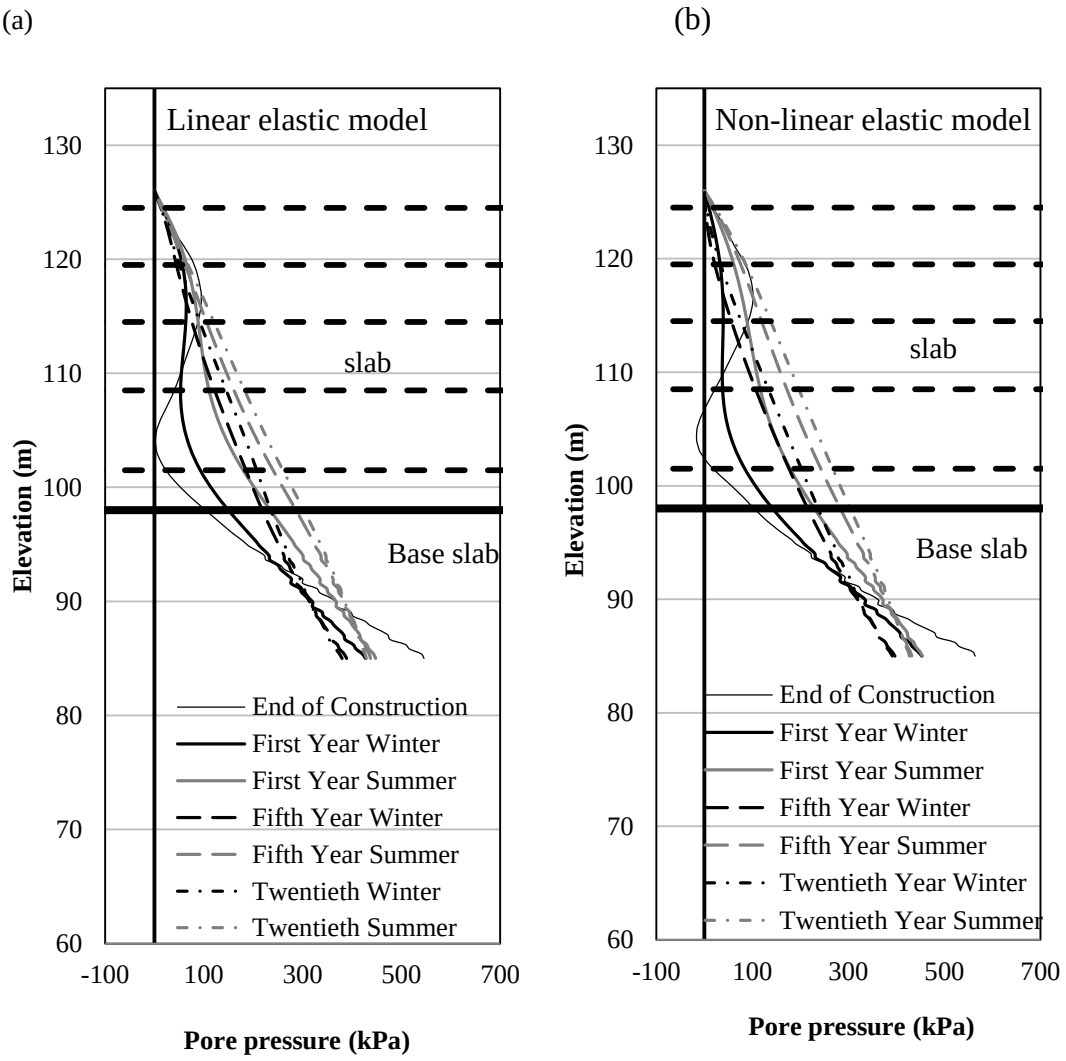

Figure 13. Comparison of pore pressure on the unexcavated side with operation of GSHP: (a) Linear elastic model; (b) Non-linear elastic model

(a) (b)

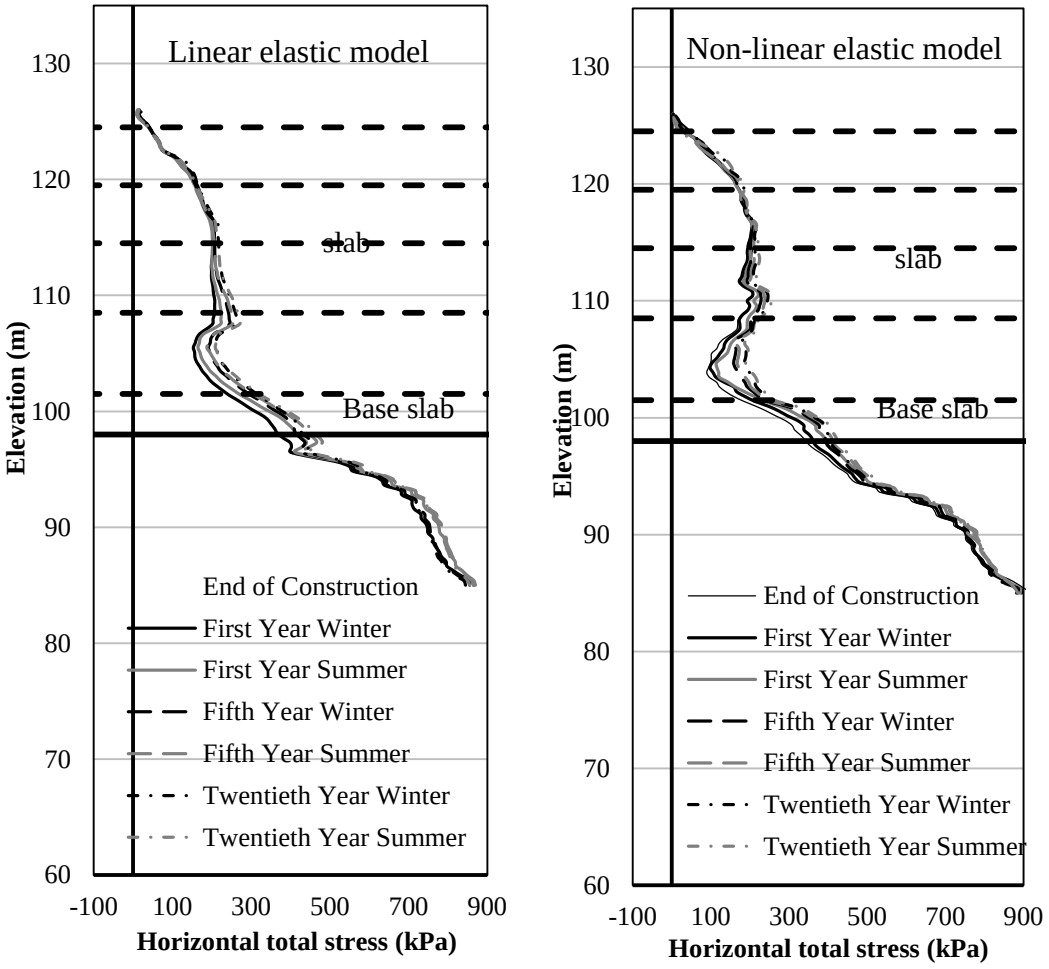

Figure 14. Horizontal total stress on the unexcavated side with operation of GSHP: (a) Linear elastic model; (b) Non-linear elastic model

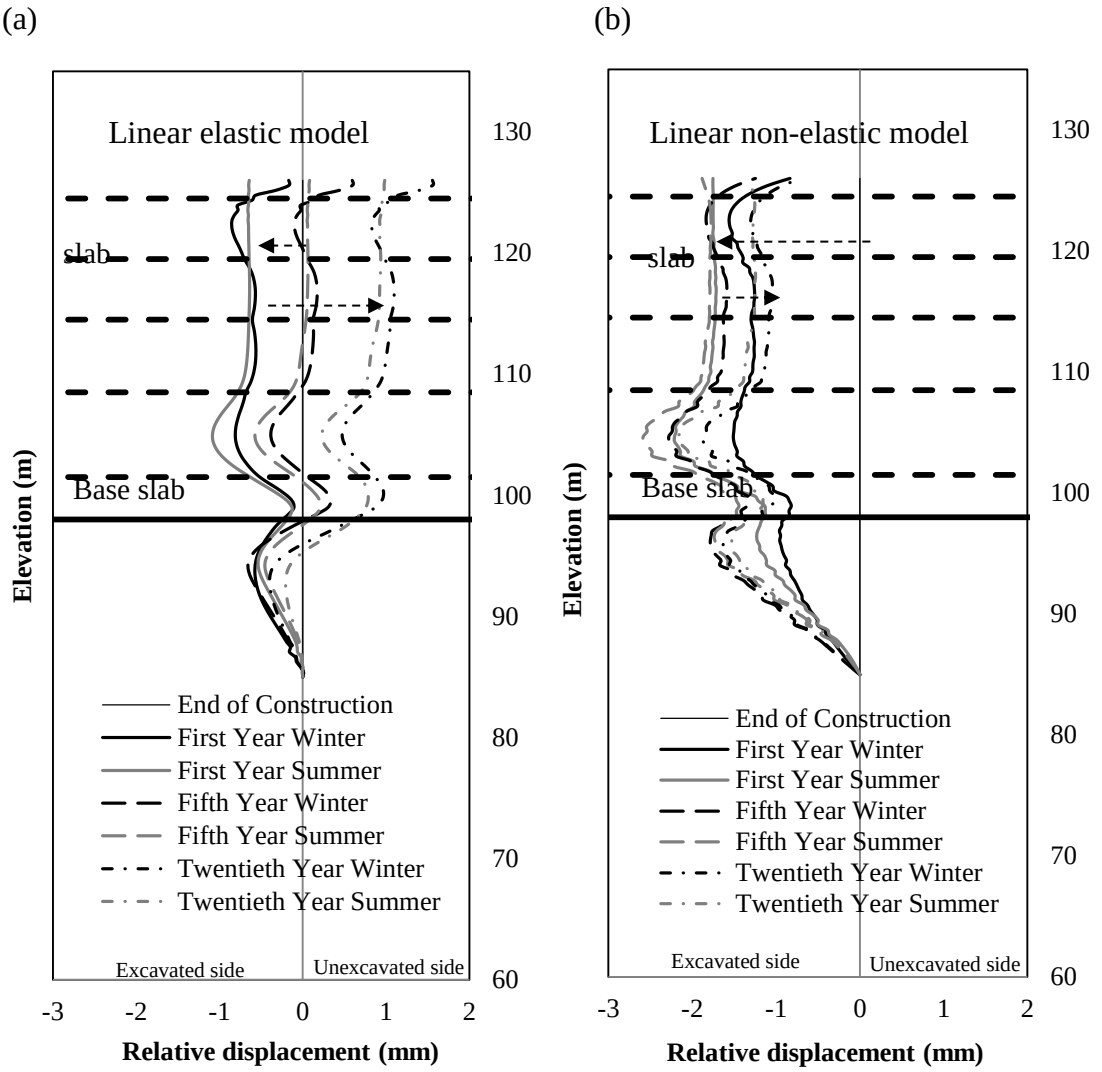

Figure 15. Relative horizontal displacement of the diaphragm wall with operation of GSHP: (a) Linear elastic model; (b) Linear non-elastic model

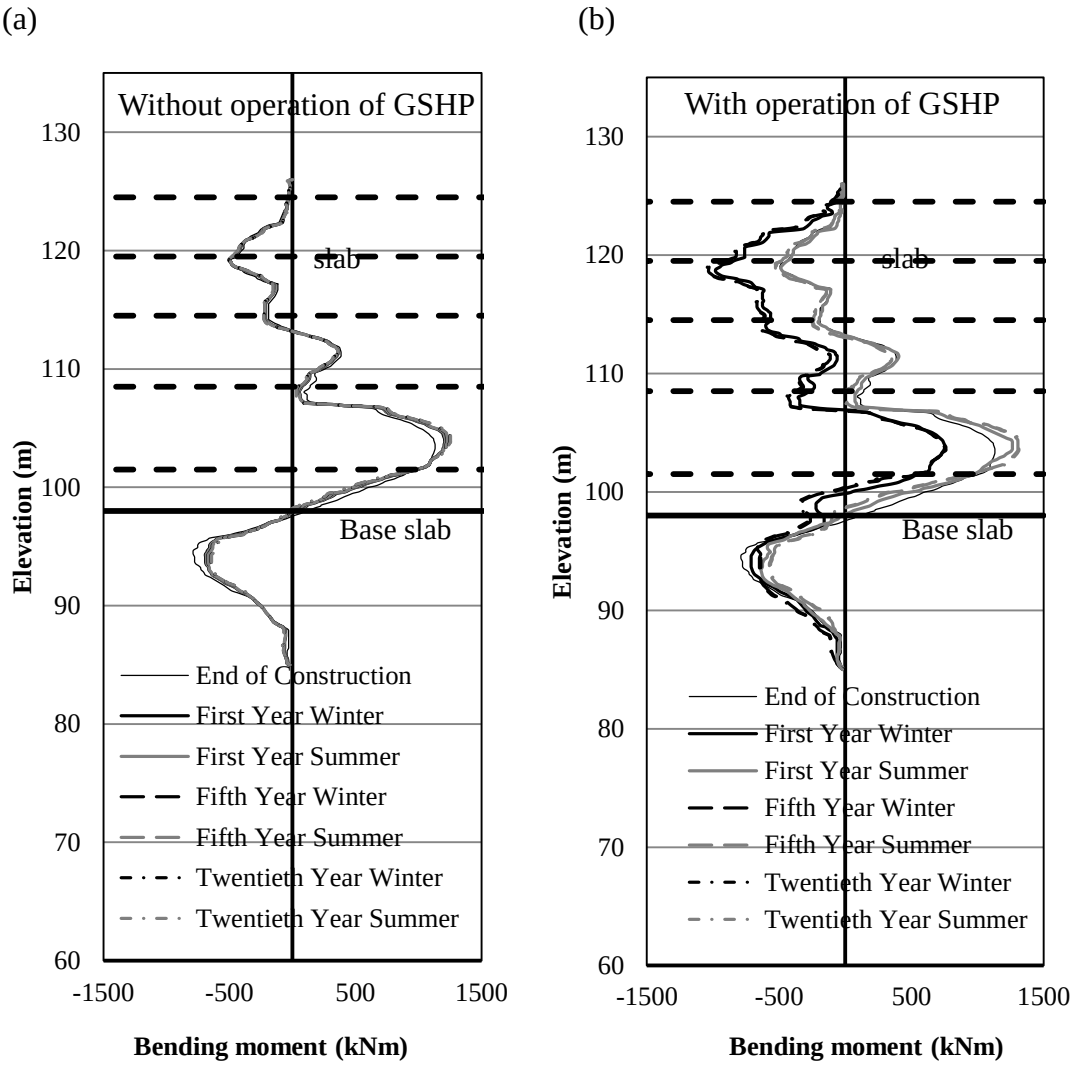

Figure 16. Bending moment of the diaphragm wall with linear elastic model: (a) Without operation of GSHP; (b) With operation of GSHP

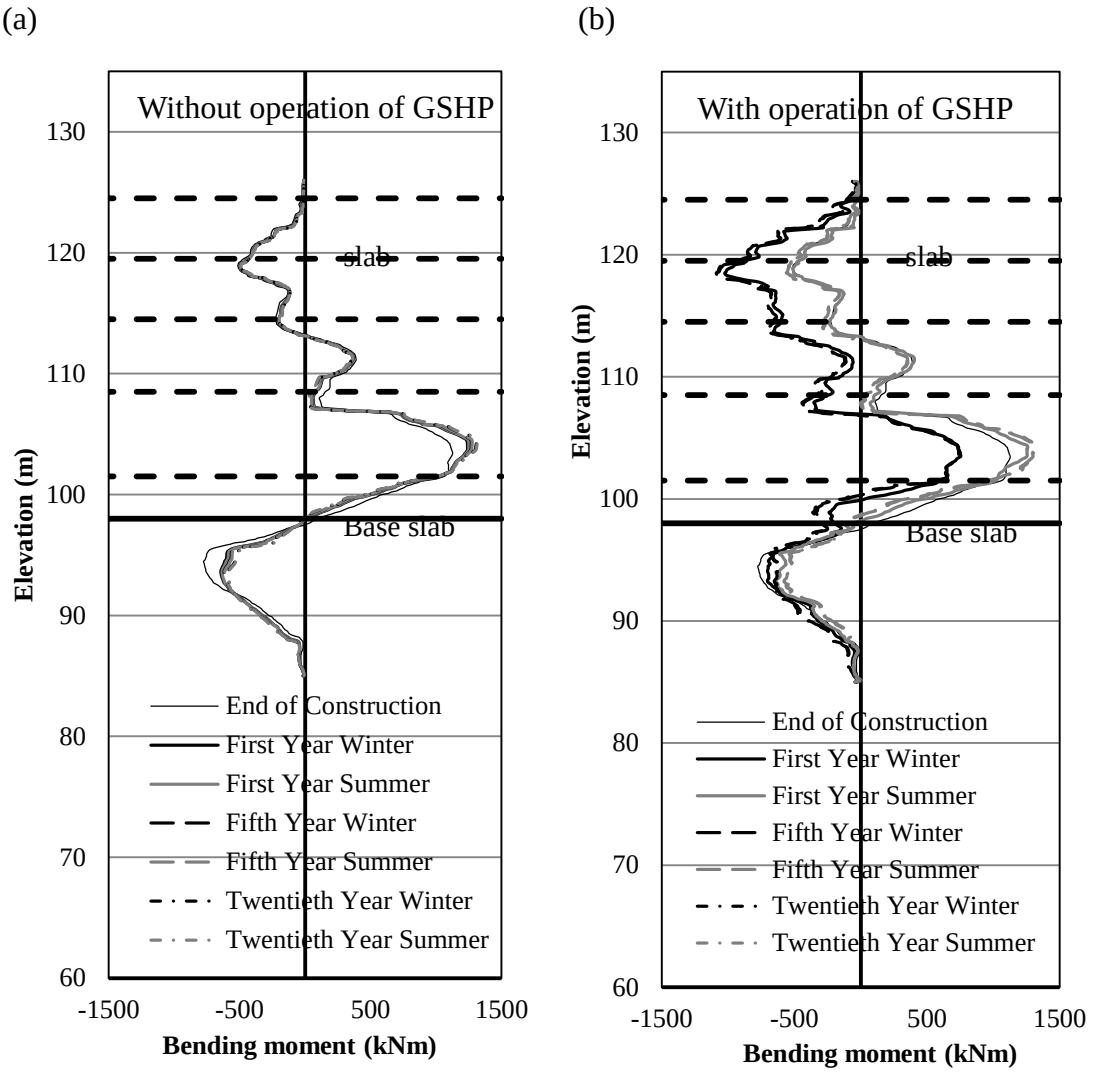

Figure 17. Bending moment of the diaphragm wall with non-linear elastic model:

(a) Without operation of GSHP; (b) With operation of GSHP

(a)

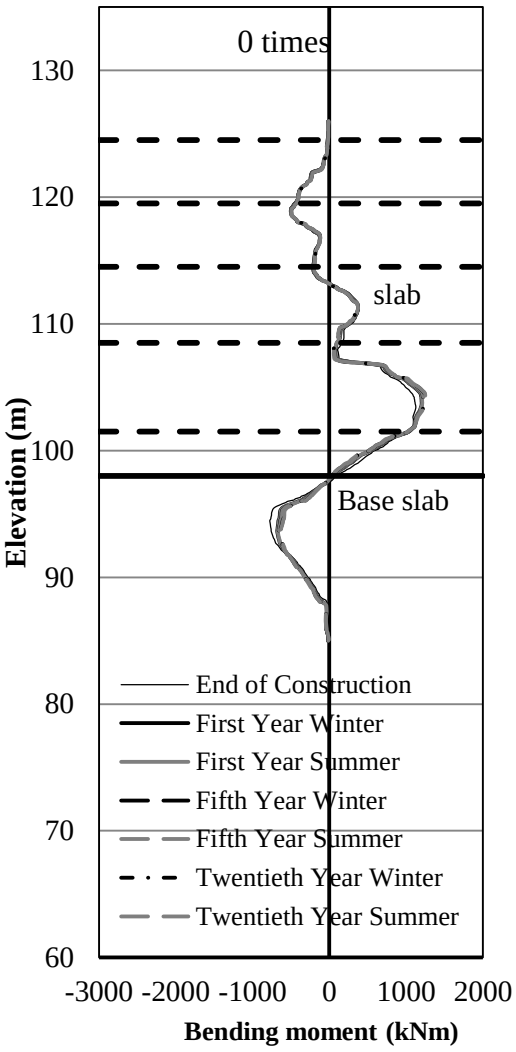
0 times
slab
Base slab
Elevation (m)
130
120
110
100
90
80
70
60
-3000 -2000 -1000 0 1000 2000
Bending moment (kNm)
End of Construction
First Year Winter
First Year Summer
Fifth Year Winter
Fifth Year Summer
Twentieth Year Winter
Twentieth Year Summer

(b)

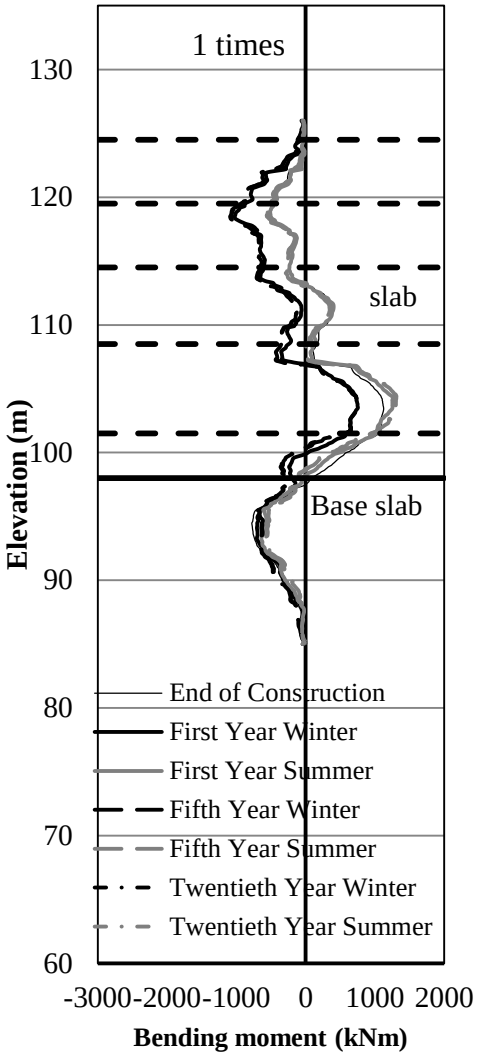
1 times
slab
Base slab
Elevation (m)
130
120
110
100
90
80
70
60
-3000-2000-1000 0 1000 2000
Bending moment (kNm)
End of Construction
First Year Winter
First Year Summer
Fifth Year Winter
Fifth Year Summer
Twentieth Year Winter
Twentieth Year Summer

(c)

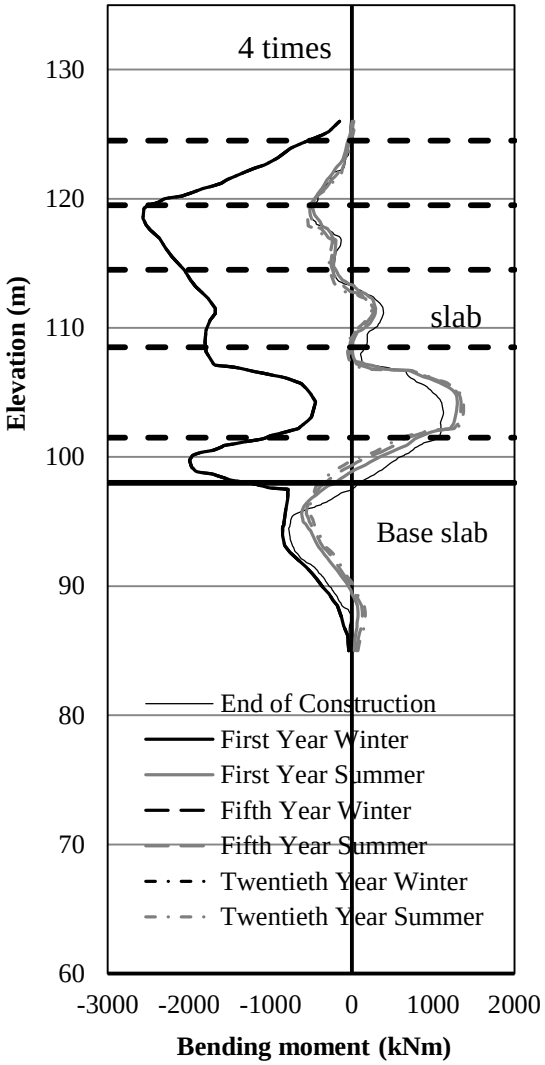

Figure 18. Bending moment of the diaphragm wall with variations in the thermal expansion coefficient of concrete: (a) 0 times; (b) 1 times; (c) 4 times